JOURNAL OF MATERIALS SCIENCE 15 (1980) 1772–1780

Creep of polycrystalline sodium chloride containing a dispersion of alumina

R. K. SINHA, J. R. BLACHERE
Department of Metallurgical and Materials Engineering, University of Pittsburgh, Pittsburgh, Pennsylvania 15261, USA

The creep of polycrystalline NaCl contaning a fine dispersion of Al_2O_3 particles is analysed in terms of dependence on stress, temperature, volume fraction and size of dispersion, and grain size of samples. Compressive creep experiments around 0.8 Tm show that the dispersion inhibits diffusive creep. The creep is characterized by a threshold stress above which the creep rate increased linearly with applied stress. The threshold stress decreases with increasing temperature and is proportional to the volume fraction of the dispersion in agreement with a model proposed by Burton. The activation energy corrected for the temperature dependence of the threshold stress falls within a narrow range consistent with grain-boundary diffusion of chlorine in sodium chloride. The grain-size dependence is not consistent with a modified diffusive creep model but it is suggested that it may be controlled by inhibited grain-boundary sliding according to a new model.

1. Introduction

The high-temperature creep behaviour of fine grain polycrystalline ceramics is generally dominated by diffusive creep mechanism [1–3] characterized by a stress exponent, n, equal to 1, an activation energy corresponding to the self-diffusion of the rate-controlling species and a strong grain-size dependence. The values of activation energy and the grain-size exponent depend upon whether the bulk diffusion [1, 2] or the grain-boundary diffusion [3] dominates the process. Ashby [4] has suggested that since both bulk diffusion and grain-boundary diffusion are present simultaneously, the diffusive creep rate may be given by an equation of the form

$$\dot{\epsilon} = \frac{B\Omega D\sigma}{d^2kT}\left(1 + \frac{B_1 wD_b}{dBD}\right) \quad (1)$$

where B and B_1 are constant, Ω is the average volume associated with monovacancies, D is the bulk diffusion coefficient, D_b the grain-boundary diffusion coefficient with w as the effective grain-boundary width, d is the average grain size, T the absolute temperature and k is the Boltzmann constant. The creep behaviour of a number of single-phase polycrystalline ceramics appears to be in excellent parametric agreement with the predominance of diffusive creep even though the absolute creep rate differs from the theoretically calculated rate by an order of magnitude [5]. The strain rate of materials containing a second-phase dispersion appears to be a few orders of magnitude lower than that of the corresponding single-phase material under similar conditions [6–9]. Relatively high values of stress exponent and activation energy of creep have been reported [7, 9] even though microstructural evidence such as the formation of denuded zones [10] suggests that the deformation is still produced by a diffusional mechanism. Another set of experiments [11–14] shows that the dispersion of second-phase particles introduces a threshold stress σ_0, below which no deformation occurs. Above the threshold stress, the strain-rate increases linearly with the stress. The strain rate then is given by Equation 1 with an effective stress ($\sigma_e = \sigma - \sigma_0$) replacing the applied stress σ.

Three different models have been proposed [15–17] to explain the existence of a threshold stress in the presence of a second-phase dispersion. All three models are based on the limitation of

0022–2461/80/071772–09$02.90/0

grain boundary as a source or sink of vacancies in the presence of particles, assuming that the deformation is still produced by diffusive creep mechanisms. The validity of these models has not been systematically tested and the relatively high values of stress exponent and activation energy of creep in the presence of a dispersion of particles have not been satisfactorily explained.

The following sections discuss the results of experiments designed to study the influence of a second-phase dispersion on the high-temperature creep of polycrystalline ceramics using $NaCl/Al_2O_3$ as a model system.

2. Procedure

Materials used for this set of experiments were NaCl* containing less than 10 ppm of cation impurities and agglomerate-free Al_2O_3† of average particle size, $2r$, equal to 0.25 and 0.06 μm, respectively. The samples were prepared by mixing and grinding NaCl and Al_2O_3 till the average particle size of NaCl was $< 1\,\mu$m. This mixture was then pressed into discs of diameter equal to ~ 30 mm and thickness ~ 11 mm. NaCl without addition was cold pressed; NaCl with dispersions were pressed at 250° C. The discs were cut into tetragons of appropriate size that were given a step-wise vacuum heat-treatment up to 450° C, followed by an annealing treatment of 48 h at $\sim 680°$ C in dry argon. All samples had densities $\sim 97\%$ theoretical.

The total cation impurities after processing was less than 100 ppm and the water picked up during processing was eliminated by the vacuum heat-treatment. The creep samples had a base of 7 mm square and a height of ~ 17 mm. The samples were crept under compression at temperatures of 580, 600 and 620° C. Stress was increased, from no load condition, in small steps until a measurable creep was observed. Temperatures were maintained constant within $\pm 0.5°$ C of the set point and measured with the same sensitivity. The stress was maintained constant by making appropriate load increments at strain intervals of 0.01.

Activation energy measurements were made by sudden upsetting of temperature ($\pm 20°$ C) at a constant applied stress. The creep samples were characterized in terms of grain-size distribution and the dispersion parameters by scanning electron microscopy of fractured surfaces as well as polished and etched sections of the creep samples.

*Puratronic NaCl, Johnson Matthey Ltd.
†Adolf Meller Co.

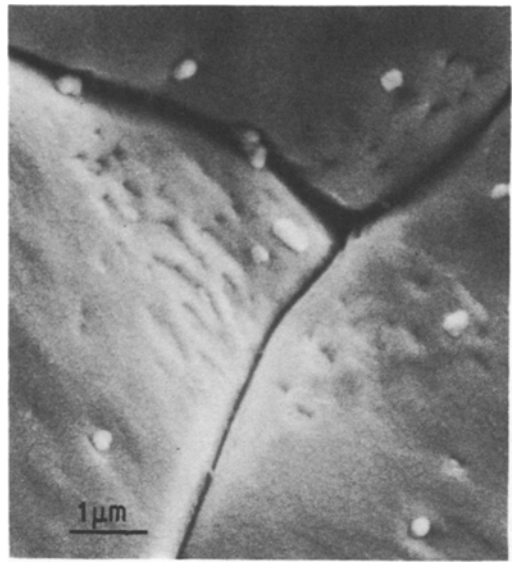

Figure 1 Dispersion of Al_2O_3 particles in NaCl sample containing 0.31 vol% 0.25 μm Al_2O_3.

3. Results

Six sets of samples were used in these experiments. One was without any alumina dispersion; three sets of samples contained 0.12, 0.31 and 0.53 vol% alumina of average particle size 0.25 μm and two sets of samples were prepared with 0.31 and 0.13 vol% alumina of particle size 0.06 μm.

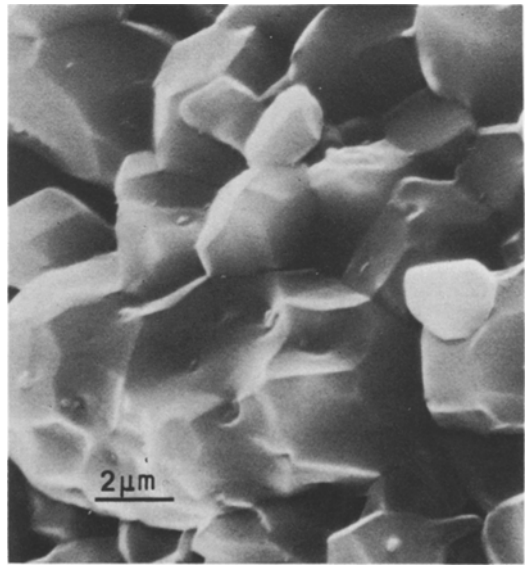

Figure 2 Intergranular fracture showing the dispersion along the grain boundaries for an NaCl sample containing 0.53 vol% Al_2O_3.

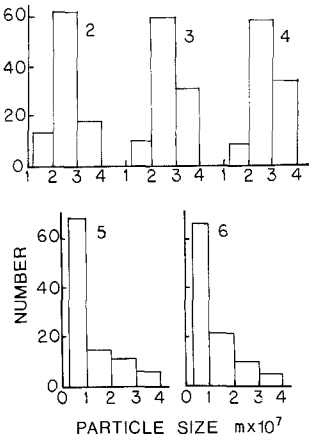

Figure 3 Particle-size distribution of alumina in samples 2 to 6.

3.1. Sample characterization

An example of the dispersion of alumina particles along an arbitrary plane is shown in Fig. 1 for the sample containing 0.31 vol% 0.25 μm Al_2O_3. Fig. 2 is a photomicrograph of a sample fractured at room temperature. It appears from the micrographs that the alumina is dispersed, in the form of individual particles as well as agglomerates of varying size, along the grain boundaries and in the interior of the grains. Since an agglomerate is expected to act as one particle, it is necessary to characterize the particle size distribution of the dispersion. Approximate distributions are shown in Fig. 3 for the samples containing Al_2O_3. Whereas the average particle size calculated from these distributions (Table I) for the coarser dispersion is a factor of ~ 3 larger than the average particle size of the fine dispersion, the largest agglomerates in both types of dispersion are of the same size.

The grain-size distribution for the sample containing no dispersion and the sample containing 0.31 vol% 0.06 μm alumina were close to log-normal. The other five samples appeared to have bimodal grain-size distributions and had to be characterized in terms of two grain sizes and the volume fraction of each grain-size fraction. The sample characterization parameters for the sample after creep are listed in Table I. No change in microstructure appeared to occur during creep. These data are used later in calculations of creep rates.

3.2. Stress dependence of creep

The stress dependence of creep rate is generally studied in terms of the stress exponent n, determined from the plot of $\dot{e}$ versus σ on a log–log scale. These plots, for the sample containing 0.13 vol% finer alumina at different temperatures, are shown in Fig. 4. The average slope, determined from the line of best fit, is 3.9 at 620° C, 4.5 at 600° C and 5.3 at 580° C. However, the slope decreases with increasing stress at each temperature. At 600° C, it is 9.4 for the line joining the two points corresponding to the lower stresses and 2.9 for that joining the two points corresponding to the higher stresses. Qualitatively similar plots were obtained for the other samples. The average slope varies from 1.6 to 6.6. In each case, the slope decreases with increasing stress. These results are summarized in Table II.

3.3. Activation energy

The apparent activation energy of creep was measured by the Dorn method for two pairs of temperatures with incremental increase and decrease of temperature. The mean values of activation energy for creep, along with 95% confidence interval, constructed using student t statistics, are plotted in Fig. 5 for all Al_2O_3 contents. The value for the sample with no dispersion is 52 ± 5 kcal mol^{-1}. However, relatively high values

TABLE I Sample characterization parameters

Sample no.	Al_2O_3 (vol %)	δ (μm)	$\bar{d}$ (μm)	F_1	d_1 (μm)	F_2	d_2 (μm)
1	0	–	37		Log-normal		–
2	0.12	0.26	5.5	0.38	8.0	0.62	3.5
3	0.31	0.27	5.5	0.66	7.0	0.34	2.5
4	0.53	0.28	4.5	0.5	6.5	0.5	2.5
5	0.31	0.11	7.5	0.5	11	0.5	4
6	0.13	0.11	15		Log-normal		–

δ = dispersion particle size after creep.
$\bar{d}$ = average grain size.
F_1, F_2 = volume fractions.
d_1, d_2 = modes of bimodal distribution of grain size.

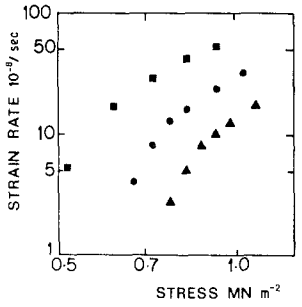

Figure 4 Variation of strain rate with the applied stress for sample 6 containing 0.06 μm Al_2O_3 (■ 650° C, ● 600° C, ▲ 580° C). Note curvature of log–log plots.

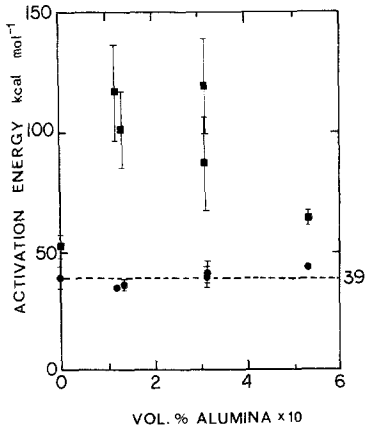

Figure 5 Apparent (■) and corrected (●) values of activation energy for creep as a function of volume fraction of Al_2O_3.

with a higher scatter are observed for the samples containing Al_2O_3 dispersions.

3.4. Grain-size dependence

Owing to the variation in the values of the apparent stress exponent and the apparent activation energy, it is not possible to make any direct comparisons to determine the grain-size dependence of creep.

4. Discussion

4.1. Microstructures

The creep samples were prepared by mixing and grinding of NaCl and Al_2O_3, pressing the powder mixture into discs and heat treating them. Care was taken to ensure that the NaCl grains at the end of grinding were of submicron size and thus smaller than the expected limiting grain size as well as the inter-particle spacing for the given amount of dispersion. After hot pressing and before the heat treatment, the Al_2O_3 particles are distributed along the grain boundaries of this fine-grained NaCl compact. The driving force for grain-boundary migration (grain growth) is estimated to be an order of magnitude higher than the retarding force due to the particles and grain boundaries migrating during the heat treatment, probably leaving the particles inside the grain. It can be shown [16] that the dispersion produced in this manner can be considered to be random and the area fraction occupied by the particles in any arbitrary cross-section is equal to the volume fraction of the particles. The distribution may be somewhat modified during the latter stages of grain-boundary migration and it can be seen in Figs. 1 and 2 that the Al_2O_3 particles and agglomerates are distributed along the grain boundaries as well as the interior of the grains, supporting the conclusion that the system can be approximated as a random distribution of Al_2O_3 in NaCl.

The role of particles in promoting secondary recrystallization has been studied by a number of workers [19, 20]. The microstructures obtained for these samples appear to have resulted from

TABLE II Conventional interpretation of creep results

Sample number	620° C			600° C			580° C			Q' (kcal mol^{-1})	Q (kcal mol^{-1})
	n_a	n_i	n_f	n_a	n_i	n_f	n_a	n_i	n_f		
1	2.0	2.7	1.8	1.6	1.8	1.5	1.8	1.9	1.7	52 ± 5	38 ± 7
2	3.9	11.8	1.3	3.4	5.4	2.6	6.2	5.0	4.8	118 ± 18	33 ± 1
3	6.6	9.7	3.0	2.9	5.6	1.5	5.8	16.0	4.1	121 ± 16	39 ± 2
4	1.7	2.1	1.4	2.0	1.6	2.7		No creep		65 ± 4	43
5	2.1	2.4	1.2	2.3	2.6	2.3	3.5	4.3	1.5	88 ± 17	39 ± 6
6	3.9	6.5	2.0	4.5	9.4	2.9	5.3	9.3	3.3	100 ± 21	34 ± 2

n_a = mean value of stress exponent.
$n_i = n$ for smaller stress.
$n_f = n$ for larger stress.
Q' = mean activation energy obtained by conventional method, along with 95% confidence interval obtained using student t statistics.
Q = mean activation energy corrected for temperature dependence of threshold stress.

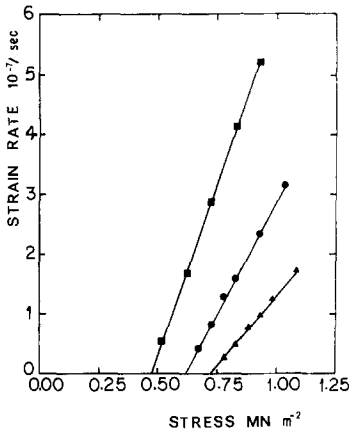

Figure 6 Strain rate versus stress plots, for sample 6, containing 0.13 vol% Al_2O_3, on a linear scale: ■ 620° C, • 600° C, ▲ 580° C.

partial (samples 2 to 5) or nearly complete (samples 1 and 6) secondary recrystallization during the preliminary heat treatment, but they did not change markedly during creep.

4.2. Stress dependence

The decrease of stress exponent, n, with increasing stress is contrary to the expected behaviour. In general, the overall creep rate is a resultant of many deformation processes ($\dot{\epsilon} = \Sigma \dot{\epsilon}_i^0 \sigma_i^n$) with different stress exponents so that the relative contribution of the mechanisms with higher n increases with increasing σ. The apparent value of n, determined from the slope of $\dot{\epsilon}$ versus σ plot on a log–log scale, will, then, be expected to increase with increasing σ. If, however, the operating creep mechanism has a threshold stress σ_0, below which no creep occurs, then the apparent value n_a of the stress exponent is given by [21]

$$n_a = n \frac{\sigma}{\sigma - \sigma_0}. \quad (2)$$

For $\sigma > \sigma_0$, n_a is always greater than n. Also as σ increases, σ_0 remaining constant, the value of n_a decreases approaching the true value of n at $\sigma \gg \sigma_0$. Thus relatively high values of the apparent stress exponent that decrease with increasing σ may be taken as suggesting a threshold stress.

The creep data was replotted on a linear scale and such a plot of $\dot{\epsilon}$ versus σ is shown for the sample containing 0.13 vol% Al_2O_3 of particle size 0.06 μm in Fig. 6. Extrapolation of the data to zero creep indicates a threshold stress. Above the threshold stress the strain rate increases linearly with σ indicating that the true value of n is 1. The threshold stress, σ_0, decreases with increasing temperature. Qualitatively similar plots were obtained for the other samples. It may be mentioned that no creep was observed at values of σ lower than

TABLE III Data of linear plots of $\dot{\epsilon}$ versus σ

Sample number	Temperature ° C	ρ	σ_0 (MN m^{-2})	$\Delta\sigma_0^*$	Fluidity Slope (m^2 MN^{-1} Sec^{-1})	Δ Slope* (m^2 MN^{-1} Sec^{-1})
	620	0.993	0.19	0.027	0.725×10^{-6}	0.12×10^{-6}
1	600	0.998	0.23	0.016	0.414×10^{-6}	0.26×10^{-7}
	580	0.998	0.29	0.023	0.267×10^{-6}	0.29×10^{-7}
	620	0.992	0.36	0.040	0.68×10^{-6}	0.1×10^{-6}
2	600	0.974	0.56	0.080	0.405×10^{-6}	0.94×10^{-7}
	580	0.984	1.07	0.010	0.26×10^{-6}	0.86×10^{-7}
	620	0.998	0.44	0.015	0.56×10^{-6}	0.44×10^{-7}
3	600	0.997	0.74	0.04	0.35×10^{-6}	0.27×10^{-7}
	580	0.988	1.24	0.14	0.2×10^{-6}	0.56×10^{-7}
4	620	0.998	0.79	0.04	0.139×10^{-6}	0.75×10^{-8}
	600	0.968	1.19	0.28	0.8×10^{-7}	0.29×10^{-7}
	620	0.996	0.64	0.07	0.15×10^{-6}	0.25×10^{-7}
5	600	0.979	1.09	0.24	0.98×10^{-7}	0.3×10^{-7}
	580	0.991	1.64	0.19	0.5×10^{-7}	0.13×10^{-7}
	620	0.999	0.475	0.01	0.115×10^{-2}	0.49×10^{-7}
6	600	0.999	0.618	0.016	0.751×10^{-3}	0.4×10^{-7}
	580	0.999	0.718	0.017	0.464×10^{-6}	0.24×10^{-7}

* 95% confidence interval constructed using student t statistics.
ρ = Linear regression correlation coefficient.

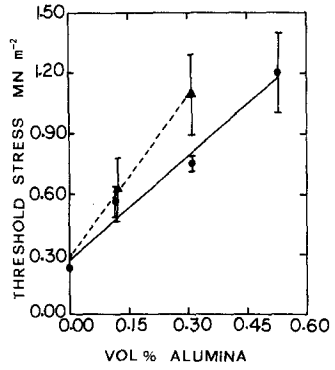

Figure 7 Variation of threshold stress with Al_2O_3 content at 600° C: ✚ $r = 0.25\,\mu m$; ▲ $r = 0.06\,\mu m$; the vertical bars represent the 95% confidence range obtained using *t*-student statistics.

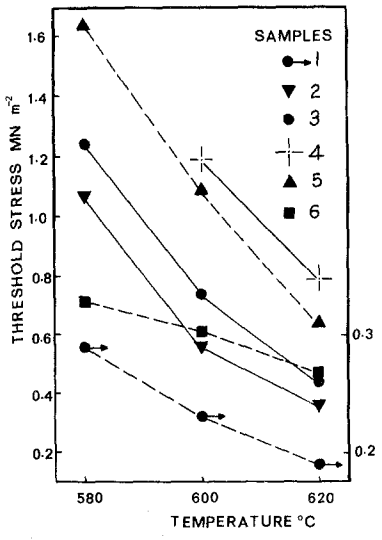

Figure 8 Temperature dependence of the threshold stress: —— 0.25 μm Al_2O_3; ---- 0.06 μm Al_2O_3; -- ✚ -- no Al_2O_3 dispersion (use right scale).

σ_0. The values of σ_0 and the slope of the linear plots for different samples at different temperatures are listed in Table III. The existence of a threshold stress, indicated by absence of creep at low stresses is supported by the observed variation of $\dot{e}$ with σ on a log–log plot and confirmed by the re-examination of the data on the linear plot.

The variation of σ_0 with the volume fraction v of the alumina is shown for 600° C in Fig. 7. The threshold stress increases linearly with v. There is a small threshold stress for the sample containing no Al_2O_3 and the slope of the line for samples containing the finer dispersion is a factor of 1.45 higher than the slope of the line for samples containing the coarser dispersion. Even though the existence of a threshold stress in a single-phase material has not been explained satisfactorily, a recent review by Pascoe [22] suggests that a number of single-phase ceramic materials* exhibit a threshold stress. The linear variation of σ_0 with v and its decrease with increasing temperature (shown in Fig. 8) can be explained only by Burton's model of threshold stress. Ashby's model [15] predicts $\sigma_0 \propto \sqrt{v}$ and does not explain the temperature dependence. Burton [17] considers the threshold stress to be associated with the nucleation of interfacial defect loops to accommodate the vacancy flux in the vicinity of particles on the grain boundary. Burton has solved the equations for this model numerically and obtained the following expression for the threshold stress

$$\sigma_0 = \frac{\pi U^2 v}{55bkT} \qquad (3)$$

*But with porosity.

where U is the line energy of the interfacial defect loop and b is the Burgers vector associated with it. Thus σ_0 is proportional to v and decreases with T. This expression, however, predicts σ_0 to be independent of the particle size, r, of the dispersion. A re-analysis of Burton's model by the authors [18] however, shows that the threshold stress associated with the nucleation of interfacial defect loops is given by

$$\sigma_0 = \frac{\pi U^2 v}{\ln (A r_c C_v r^3) \cdot bkT} \qquad (4)$$

where $A = 8\pi b^2/(3\Omega^2)$ is a constant, r_c is the critical loop radius above which the loops can grow spontaneously and C_v is the equilibrium vacancy concentration. The ln term complicates the temperature dependence but it is a constant for a given system at a given temperature, and does not seem to vary rapidly with temperature (Fig. 8). The value of this term increases by a factor of about 1.4 for r changing by a factor of 4. Thus the observed increase in σ_0 (of 45%) versus the change in r is in approximate agreement with that predicted by Equation 4. The variation of σ_0 with v, T and r, hence, appears to be consistent with this analysis of Burton's model for a threshold stress.

4.3. Activation energy measurements

The conventional measurements of activation energy were made using the Dorn method that is based on the assumption that the stress and tem-

perature dependence of the strain rate can be expressed as

$$\dot{\epsilon} = A\, e^{-Q'/RT} \tag{5}$$

so that the activation energy is given by

$$Q' = -R \frac{\mathrm{d}(\ln \dot{\epsilon})}{\mathrm{d}(1/T)}. \tag{6}$$

If, however, the predominant creep mechanism has a temperature-dependent threshold stress, the strain rate is given by

$$\dot{\epsilon} = A'[\sigma - \sigma_{0(T)}]^n e^{-Q/RT}.$$

Since $\sigma > \sigma_0$ and the threshold stress decreases with increasing temperature, as observed here, then $\mathrm{d}\sigma_0/\mathrm{d}T$ is negative so that Q' is always larger than the actual value of Q. Hence, the conventional treatment of data can give large values of apparent activation energy if the temperature dependence of the threshold stress is not taken into account.

For a mechanism where n is equal to 1, the correct value of Q can be determined using the fluidity defined by $1/\eta_c = \dot{\epsilon}/(\sigma - \sigma_0)$ instead of $\dot{\epsilon}$ so that the activation energy is given by

$$Q = -R \frac{\mathrm{d} \ln [\dot{\epsilon}/(\sigma - \sigma_0)]}{\mathrm{d}(1/T)}.$$

The fluidity for a sample at a given temperature is equal to the slope of $\dot{\epsilon}$ versus σ plot on a linear scale. The activation energy determined from this modified equation falls in the range of 39 ± 7 kcal mol^{-1} for all the samples and is also plotted in Fig. 5. This value of activation energy is in very good agreement with the value reported for the grain-boundary diffusion of Cl^- in NaCl [26]. This is consistent with the grain-boundary diffusion mechanism of creep that is expected to be predominant under the given experimental conditions [26].

4.4. Grain-size dependence

Having determined the value of the stress exponent ($n = 1$) and the corrected activation energy ($Q = 39 \pm 7$ kcal mol^{-1}), it is now possible to determine the grain-size dependence of the creep rate by comparing the fluidity of the different samples at a given temperature. A plot of the fluidity against grain size is shown in Fig. 9. The solid line was calculated using Equation 1 with $\sigma - \sigma_0$ replacing σ. For the samples with a bimodal distribution of grain sizes the effective average grain size given in Table I was used. It was calculated from the grain-size distribution (Table I) with the equation $\bar{d} = (F_1 d_1^3 + F_2 d_2^3)^{1/3}$ in an

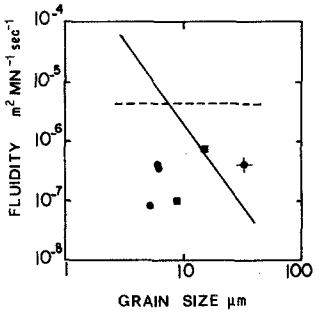

Figure 9 Variation of the fluidity with the grain size for NaCl samples ✦ no dispersion, • coarse Al_2O_3 dispersion, ▪ fine alumina dispersion, —— diffusive creep, ---- grain-boundary sliding.

adaptation to grain-boundary diffusion mechanisms of the treatment of Burton [5] for Nabarro–Herring creep of samples with bimodal distribution of grain sizes. The value for the sample containing no dispersion agrees with the theoretically calculated value within an order of magnitude, the experimental value being larger by a factor of ~ 6. The fluidity for the samples containing dispersions of Al_2O_3 is, however, relatively insensitive to the grain size as opposed to a strong grain-size dependence expected for diffusive mechanisms. Thus the values of n and Q indicate the possibility of grain-boundary diffusion mechanism of creep but the grain size dependence does not agree with this model.

It may be recalled here that diffusional deformation is always accompanied by grain-boundary sliding and the total process may be viewed either as diffusional creep with incompatibilities accommodated by grain-boundary sliding [23, 24] or as grain-boundary sliding with the incompatibilities accommodated by diffusion [25]. The slower of the two processes will be rate-controlling. Ashby [4] has shown that the rate of deformation by sliding of grain boundaries (in absence of irregularities) is a few orders of magnitude faster than the rate of diffusional deformation. Raj and Ashby [25] have shown that in the presence of irregularities or over a dispersion of particles on the grain boundaries, the rate of sliding is still fast enough for the rate of creep to be controlled by the diffusive accommodation of material around the irregularities (particles). This assumption may, however, not be valid when a dispersion of closely spaced (small interparticles distance λ) particle of large size ($2r$) is present on the grain boundaries. If grain-boundary sliding is due to the glide of grain-boundary dislocations in the plane of the

boundary, then, in the presence of particles on the grain boundary, the dislocations may have to climb over the particles for continuous grain-boundary sliding to take place. A model for particle-inhibited grain-boundary sliding [18] shows that the sliding step, controlled by the grain-boundary dislocation climb over the particle, will become rate-controlling if

$$b\lambda^2 d^2 < 150\, r^5 \tag{10}$$

where b is the Burgers vector associated with grain-boundary dislocation, and λ is the inter-particle distance. The creep rate is given by

$$\dot{\epsilon} = \frac{2}{\pi} \cdot \frac{b\lambda^2 w D_b \Omega\sigma}{dr^5 kT}. \tag{11}$$

If the grain size d follows a Zener type relation so that

$$d = \frac{A'r}{v}, \tag{12}$$

where A' is the constant relating the average grain size to the average radius of curvature of the boundary, and $\lambda = r\sqrt{(2\pi/3v)}$ for random distribution of particles, then λ^2/d is a constant and $\dot{\epsilon}$ will become independent of the grain size. Even if d does not follow Equation 12 exactly, the strain rate, for random distribution of particles is given by

$$\dot{\epsilon} = \frac{4}{3} \frac{bwD_b \Omega\sigma}{dvkTr^3} \tag{13}$$

and since d decreases as v increases, the strain rate will appear to be insensitive to these variables.

A stress exponent of 1, an activation energy corresponding to D_b and $\dot{\epsilon}$ insensitive to the grain size obtained in this study are in agreement with this model of diffusive creep controlled by particle-inhibited grain-boundary sliding. However, this model predicts a strong dependence of $\dot{\epsilon}$ on the particle size r that is not observed experimentally. Since the dislocations have to climb over all the particles in the dispersion, the climb over the largest particles (or agglomerates) will be rate-controlling. Examining the particle-size distribution in the creep specimen, it can be seen that the largest size was the same in both types of dispersion and hence the same value of r should be used for the two. Further, the dependence of $\dot{\epsilon}$ on the particle size may be difficult to determine in future experiments since, for small particles the inhibition of grain-boundary sliding is not effective and the diffusion step may be rate-controlling and for large particles, grain-boundary sliding may be completely suppressed and some other, non-diffusive, mechanism may dominate the creep behaviour.

It may also be noted that even though the particle-inhibited grain-boundary sliding may be the rate-controlling step, diffusion is still an integral part of the process and hence the model is consistent with the explanation given for the threshold stress.

5. Conclusions

It may be concluded from the foregoing discussion of the experimental results on the creep of sodium chloride samples that the diffusive creep in sodium chloride is inhibited by a dispersion of Al_2O_3 particles. This inhibition is characterized by a threshold stress below which no creep occurs. Above the threshold stress, the strain-rate increases linearly with the applied stress implying that the correct value of the stress exponent is 1. The relatively high values of n and Q given by the conventional treatment of the data, and their variation, were explained successfully in terms of this threshold stress and its temperature dependence. The corrected value of activation energy falls in the range of 39 ± 7 kcal mol^{-1} that corresponds to the grain-boundary diffusion of Cl^- ions in NaCl. The variation of σ_0 with v, T and r is consistent with a refined analysis of Burton's model.

The values of n and Q suggest the possibility of a grain-boundary diffusion mechanism being dominant. However, the creep behaviour is insensitive to any variation in the grain size of the material as opposed to a strong grain-size dependence expected for the diffusive mechanism. This may be explained by grain-boundary sliding inhibited by the second-phase particles.

The interpretation of the data for n and Q has great significance for the creep of many polycrystalline ceramics for which stress exponents are somewhat greater than one. In many materials, in particular those containing a second-phase dispersion, unreasonably large activation energies are reported in the literature. It has been shown in this research that taking into account the temperature dependence of the threshold stress the activation energy for creep is consistent with that of the controlling transport process.

In future investigations of the creep of polycrystalline ceramics with or without second-phase

dispersions, the possibility of a threshold stress should always be investigated in detail.

Acknowledgement

This research was supported in part by the National Science Foundation DMR Grant no. 76-17780.

References

1. F. R. N. NABARRO, in "Report of a Conference on the Strength of Solids" (Phys. Soc. London, 1948) p. 75.
2. C. HERRING, *J. Appl. Phys.* **21** (1950) 437.
3. R. L. COBLE, *ibid.* **36** (1963) 2412.
4. M. F. ASHBY, *Surface Sci.* **31** (1972) 498.
5. B. BURTON, "Diffusional Creep of Polycrystalline Materials" (trans. Tech. Publications, Aedermannsdorf 1977).
6. L. E. RARATY, *J. Nucl. Mater.* **20** (1966) 344.
7. P. GREENFIELD and W. VICKERS, *ibid.* **22** (1967) 77.
8. W. VICKERS and P. GREENFIELD, *ibid.* **24** (1967) 249.
9. *Idem, ibid.* **27** (1968) 73.
10. R. L. SQUIRES, R. T. WEINER and M. PHILLIPS, *ibid.* 8 (1963) 77.
11. F. K. SAUTTER and E. S. CHEN, in "Oxide Dispersion Strengthening" (Gordon and Breach, New York 1966) p. 495.
12. B. BURTON, *Met. Sci. J.* **5** (1971) 11.
13. J. R. BLACHERE, *Amer. Ceram. Soc.*
14. R. K. SINHA, M.S. Thesis, University of Pittsburgh (1977).
15. M. F. ASHBY, *Scripta Met.* **3** (1969) 837.
16. J. E. HARRIS, *Met. Sci. J.* **7** (1973) 1.
17. B. BURTON, *Mat. Sci. Eng.* **10** (1972) 9.
18. R. K. SINHA, Ph.D. Thesis, University of Pittsburgh (1978).
19. J. E. MAY and D. TURNBULL, *Trans. Met. Soc. AIME* **212** (1958) 769.
20. T. GLADMAN and F. B. PICKERING, *J.I.S.I.* **2051** (1967) 653.
21. R. K. SINHA and J. R. BLACHERE, *Scripta Met.* **13** (1979) 41.
22. R. T. PASCOE, Central Electricity Laboratory, Lab. Memo no. R.D/L/M 342, Job no. VM 274 (1971).
23. G. B. GIBBS, *Mat. Sci. Eng.* **2** (1968) 269.
24. T. M. LIFSHITZ, *Sov. Phys. J.E.T.P.* **117** (1963) 909.
25. R. RAJ and M. F. ASHBY, *Met. Trans.* **2** (1971) 1113.

Received 24 October and accepted 5 November 1979.